NASA TECHNICAL MEMORANDUM

NASA TM X-1310

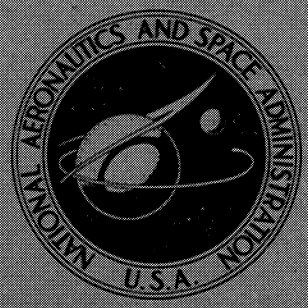

NASA TM X-1310

EXPERIMENTAL FEASIBILITY STUDY OF WATER-FILLED CAPILLARY-PUMPED HEAT-TRANSFER LOOPS

by Francis J. Stenger

Lewis Research Center

Cleveland, Ohio

NATIONAL AERONAUTICS AND SPACE ADMINISTRATION • WASHINGTON, D. C. • NOVEMBER 1966

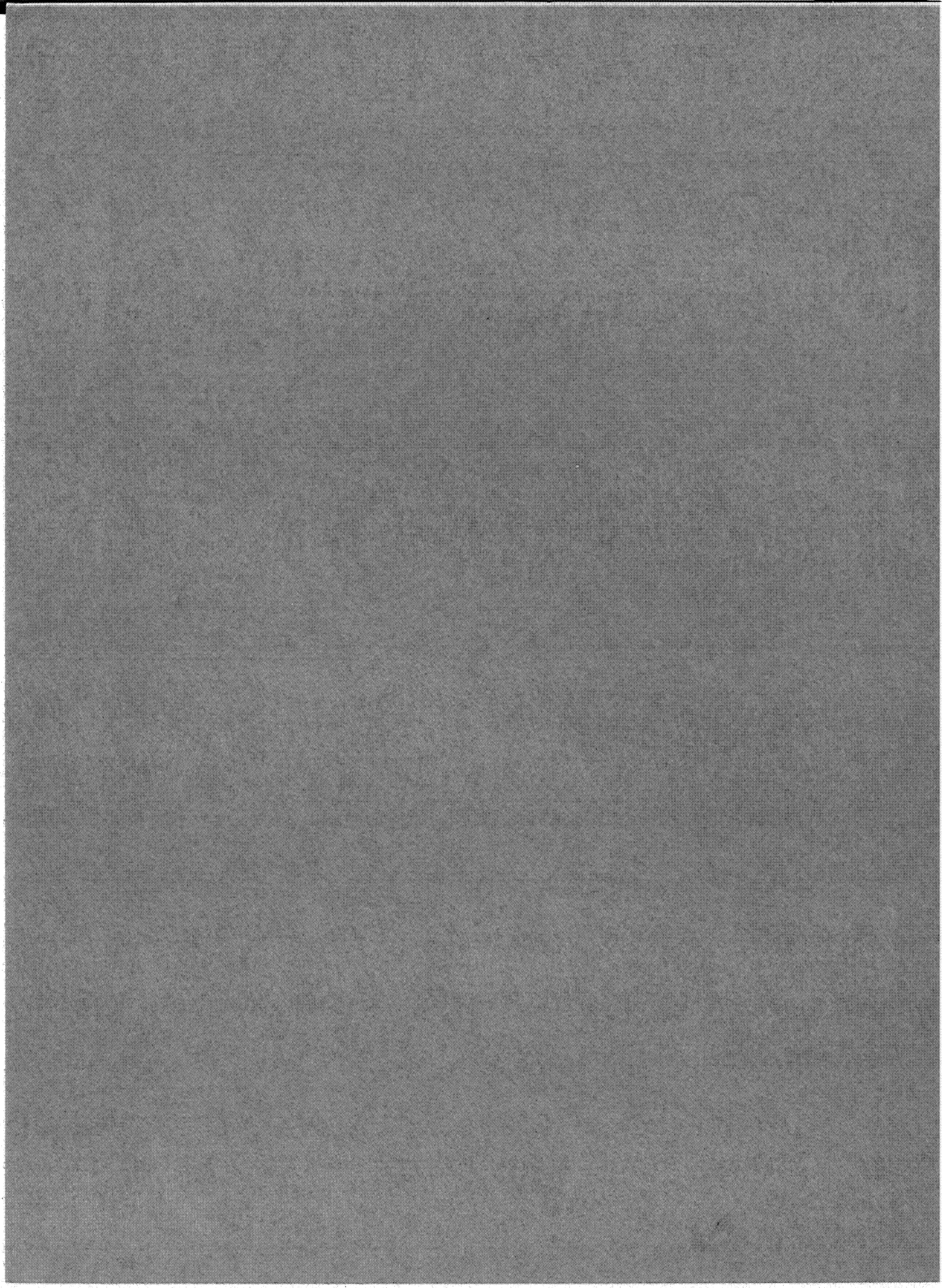

NASA TM X-1310

EXPERIMENTAL FEASIBILITY STUDY OF WATER-FILLED CAPILLARY-PUMPED HEAT-TRANSFER LOOPS

By Francis J. Stenger

Lewis Research Center
Cleveland, Ohio

NATIONAL AERONAUTICS AND SPACE ADMINISTRATION

For sale by the Clearinghouse for Federal Scientific and Technical Information
Springfield, Virginia 22151 – Price $2.00

EXPERIMENTAL FEASIBILITY STUDY OF WATER-FILLED CAPILLARY-PUMPED HEAT-TRANSFER LOOPS

by Francis J. Stenger

Lewis Research Center

SUMMARY

Two capillary-pumped heat-transfer loops were fabricated and tested to study their general characteristics. With water as a working fluid, the loops were operated over a power input range from 248 to 1000 watts in a temperature range from 212° to 291° F. The first loop, with a vapor duct 0.193 inch in inside diameter, was 70 feet long and operated at a maximum power input of 823 watts. The second loop (0.180-in. i.d. vapor duct) was 52 feet long and operated at 700 watts in a variety of orientations with respect to gravity.

Although capillary-pumped loops must be designed with care to prevent problems with noncondensable gas, the test results show that such loops can transfer kilowatts of heat over distances greater than 50 feet. The operation of the final test loop was not sensitive to its orientation with respect to gravity.

INTRODUCTION

Space power devices such as fuel cells, batteries, thermionic diodes, etc., must transfer waste heat to radiators for dissipation to space. In small units (of a few hundred watts output) the waste heat can be rejected by conduction through solid members. In larger devices, conduction as a means of transferring heat to the radiator will likely be inadequate because of the combination of large thermal powers and long conduction paths. Heat-transfer loops employing circulating working fluids will then be required. Although the fluids in these loops can be made to circulate by using electrically or mechanically driven pumps, such pumps consume valuable system power and add to system complexity. To aggravate the problem further, the meteoroid environment of space makes it desirable to construct a space radiator in many individually pumped segments rather than as one large unit (ref. 1). Thus, any simple, non-power-consuming pumping mechanism for

application to heat-transfer loops is of interest for space systems.

One method of achieving fluid motion and heat transfer in a loop without using an externally powered pump has recently been investigated. The device, called a "heat pipe" (refs. 2 to 4), is essentially a closed duct with a capillary structure, that is, a wick, covering the inner walls. A quantity of two-phase working fluid is contained in the duct - liquid in the wicking structure and vapor in the remaining volume. The duct automatically tends to maintain itself at a uniform temperature by the mechanism of liquid vaporization in the hot areas and vapor condensation in the cool areas. Liquid is moved within the wick structure, against the current of the vapor flow, from the condensation areas to the evaporation areas by means of capillary pumping (surface-tension forces). Present heat pipes usually use wicks in which the pore size is uniform over the entire length of the duct. This wick uniformity requires that a compromise be made in selecting the wick pore size. On the one hand, it is desirable to use a small-pore wick to maximize the capillary pumping pressure difference and to minimize the effect of gravity on the liquid in the duct. However, this small-pore requirement conflicts with the need to keep the wick pores large enough to transport the working liquid the full length of the duct without incurring an excessive liquid pressure drop. What is needed is a system wherein the pumping function of the wick is separate from the liquid-transport function.

In the capillary-pumped loops tested for this report an attempt was made to restrict the small-pore pumping wick to the evaporator section of the loop and to limit the capillary structure of the loop's condensing portion to no more than the smooth walls of the condensing tube itself. A condenser duct diameter was selected that would permit a liquid slug to bridge and plug the duct even in a 1-g environment. If surface tension would stabilize the free ends (liquid-vapor interfaces) of the slugs, then the slugs might be moved downstream like a piston in a cylinder, subject to a pressure differential generated across the hot surface of the fine-pore pumping wick in the evaporator. The fine-pore pumping wick would be very short and thus, a large liquid-phase pressure drop would be avoided. If the slug flow mechanism were active in the loop condenser, the loop should perform in a 1-g environment much as it would in a zero-gravity state, and ground tests could be used to checkout a system designed to operate in space.

To study the feasibility of such capillary-pumped heat-transfer loops an experimental program was conducted at the Lewis Research Center. This report covers the experimental work performed and contains a general discussion of the principle of operation of the test loops. More background on capillary pumping may be obtained from the capillary-pumped vapor generator work of Laub and McGinness in references 5 and 6, and from the heat pipe theory of Cotter in reference 4. Two water-filled loops of the following configurations were investigated:

(1) A coaxial copper evaporator with a glass-tube condenser of variable length

(2) A coaxial nickel evaporator with a stainless-steel-tube condenser of constant length

The investigation was of an exploratory nature for the purpose of determining the feasibility of these loops as heat-transfer devices. The experimental results are therefore indicative of general loop mechanisms rather than a rigorous definition of the internal fluid dynamic and heat-transfer characteristics.

SYMBOLS

C_p specific heat of working fluid liquid, Btu/(lb mass)(^oF)

D_p wick pore diameter, ft

D_t inside diameter of condenser tube, ft

E total power input to evaporator (1000 W = 0.948 Btu/sec), Btu/sec

h_{fg} latent enthalpy of vaporization, Btu/lb mass

L_p length of wick pore, ft

m working fluid flow rate, lb mass/sec

N_p total number of wick pores

ΔP_e pressure rise across capillary evaporator, lb force/ft^2

r radius of curvature of menisci in wick pore exits, ft

Re Reynolds number

ΔT_e temperature difference between average evaporator outer surface temperature T_s and saturated vapor temperature at evaporator outlet T_o, ^oF

ΔT_ℓ ^oF of feed liquid subcooling

T_o saturated vapor temperature at evaporator outlet, ^oF

T_s average evaporator outer surface temperature, ^oF

v_f specific volume of liquid water, ft^3/lb mass

μ_v dynamic viscosity of working fluid vapor, (lb force)(sec)/ft^2

σ surface tension of working fluid, lb force/ft

Station numbers for schematic model of evaporator:

1 vapor side of vapor-liquid interface in condenser

2 liquid side of vapor-liquid interface in condenser

3 liquid immediately upstream of wick entrance

4 wick entrance

4* point in wick where liquid changes from subcooled to superheated state

5 liquid immediately upstream of wick exit (boiling surface)

6 wick exit

7 vapor immediately downstream of wick exit

PRINCIPLE OF OPERATION

General Concept

The basic concept of a capillary-pumped heat-transfer loop is illustrated in figure 1. The model loop consists of two main sections, the evaporator or heat-input section and the condenser or heat-rejection section. The evaporator performs the following functions:

(1) Provides a heat-input surface through which the waste heat source rejects its heat load

(2) Transfers the waste heat load to the working fluid by vaporizing the working fluid

(3) Pumps the working fluid around the loop by capillary action at the wick evaporation surface

The condenser section of the loop:

(1) Rejects the waste heat load to the heat sink by condensing the fluid vapor

(2) Provides a duct to return the liquid condensate to the evaporator inlet

(3) Subcools the liquid condensate to provide a "net positive suction head" at the evaporator inlet

Another important component of the loop is the working fluid. It must have the thermodynamic, fluid dynamic, and chemical characteristics to provide the heat-transfer performance and operating life required of the loop.

Pumping Mechanism

The following discussion considers the pumping mechanism, the condensate return mechanism, and the working fluid requirements in more detail.

Fluid-cycle detail. - The condensing interface and wick section of an idealized capillary-pumped heat-transfer loop are shown in figure 2. The condensing portion of the duct that would close the loop is not shown. The duct is assumed to be a round tube of inside diameter D_t. The wick section is cylindrical, of length L_p, with a number of

axial holes (pores) N_p, and fit with zero radial clearance into the large flow duct between stations 4 and 6 (fig. 2(a)). The duct contains a two-phase pure-component working fluid with a vapor-liquid interface at station 1, a continuous liquid phase from station 2 to station 5, and a liquid-vapor interface in the wick exit at station 6. The liquid is assumed to wet the solids in the duct with zero contact angle. The remainder of the loop from station 7 to 1 contains a mixture of vapor and condensate moving toward station 1.

The operating principle of the loop may be visualized by tracing a fluid element around one circuit of the duct. Beginning with saturated liquid at duct station 2, a liquid element subcools by rejecting heat through the duct wall to the surroundings. This subcooling continues until the liquid reaches a minimum temperature at station 3 just before it enters the wick structure. After the liquid passes station 3, the temperature of the fluid element starts to rise as it begins to absorb the heat load being conducted to it from the heat-input surface at station 6. The temperature of the liquid continues to rise as it moves through the wick pores to station 5. Liquid at station 5 moves through the heat-input surface at station 6, takes on its latent heat of vaporization, and is changed to the vapor phase at station 7. Because of the highly curved liquid-vapor interfaces (menisci) in the wick pore exits (between stations 5 and 6) and the surface tension of the liquid, the vapor at station 7 is at a higher pressure than the liquid at station 5 (refs. 5 and 6). The pressure difference between stations 5 and 7 provides the motive force to move the working fluid around the loop. The vapor moves through the condensing portion of the duct from station 7 to station 1, gives up its latent heat of vaporization to the surroundings, and changes to a continuous liquid phase by the time it reaches station 2 to begin another circuit of the loop.

Figure 2(b) shows the general trends of the fluid pressure and temperature profiles along the model in figure 2(a). It is assumed that the heat-transfer rates in the condensing portion of the duct are low enough that the fluid vapor and liquid are very near saturated conditions. The fluid pressure must drop across the vapor-liquid interface between stations 1 and 2. This pressure drop will be equal to $4\sigma_2/D_t$, where σ_2 is the surface tension of the liquid at station 2 and D_t is the local duct diameter. Thus, the curvature of the liquid-vapor interfaces at the wick pore exits (station 6) must be such that the pressure rise from station 5 to station 7 equals the total fluid friction pressure drop around the duct, plus the $4\sigma_2/D_t$ pressure drop from station 1 to station 2. The pressure rise from station 5 to station 7 will have a magnitude of $2\sigma_5/r$, where r is the radius of curvature of the interfaces in the pore exits and σ_5 is the surface tension of the liquid at station 5. The maximum value of this capillary pressure rise is the bubble pressure of the wick, or $4\sigma_5/D_p$, where D_p is some effective wick pore diameter. The bubble pressure as used in this report is simply that pressure difference required to force vapor through a liquid-filled wick. Thus, the maximum condenser pressure drop the evaporator can sustain is $4(\sigma_5/D_p - \sigma_2/D_t)$ (assuming a zero contact angle).

From figure 2(b), it is observed that at some station within the wick structure, for

example, station 4*, the liquid must go from a subcooled to a superheated state. As the feed liquid to the wick inlet (station 4) is subcooled more and more, the position of station 4* will move nearer to station 6. With less subcooling, station 4* will move upstream toward station 4. If the liquid is not subcooled enough, it may become superheated before it enters the wick pores and the net positive suction head of the evaporator, considered as a pump, would be zero. Operation of the wick as a pump under these conditions may not be possible. The specific amount of subcooling required for an actual evaporator is a complex function of the working fluid, the duct and wick material and geometry, and the noncondensable gas content of the duct.

Wick structure requirements. - The wick structure must have specific characteristics to meet the pumping requirements of the loop. First, the geometry of the wick must provide the correct pore size. If the wick pores are too small, the liquid flow resistance in the pores may be excessive, even though the pressure difference the wicking forces can support is relatively large. On the other hand, if the wick pores are too large, the liquid flow resistance will be low, but the wick capillary forces may not be able to support the required pressure differential. In other words, the detailed wick characteristics, such as pore size and overall wick thickness, must be matched to the specific pumping requirements of a particular loop. Some of the considerations necessary for selecting a good wick design are analyzed by McGinness and Laub in references 5 and 6.

Wick boiling surface. - All three important functions (heat input, fluid vaporization, and fluid pumping) of the evaporator occur near the wick boiling surface region. At station 6 in figure 2(a), it is assumed that some arrangement exists for conducting a heat load to the exposed wick surface and for venting the effusing vapor into the flow duct at station 7. In practice, this dual function of the boiling surface is realized by using some form of extended metal lattice in contact with the wick surface. Continuous metal paths between the heat source and the wet wick carry heat to the liquid-vapor interface, while grooves or channels are provided to vent the resulting vapor flow into the vapor duct. A more detailed description of boiling surface characteristics is reserved for later discussion of specific evaporator design.

Condensate Return Mechanism

During steady-state operation of a capillary-pumped loop, the liquid portion of the working fluid moves around the loop in three different flow regimes: initially, as an annular film covering the wall of the condenser duct, then as a succession of slugs separated by condensing vapor bubbles, and finally, as an all-liquid phase. In general, all three flow regimes will exist in a given loop at the same time.

The relatively high-velocity vapor flowing from the evaporator outlet causes the con-

densate to first be transported along the wall as a film. This film moves along the duct wall as a result of the viscous drag between the film and the faster moving central vapor core. However, where the vapor velocity is low, surface-tension effects begin to control the mode of condensate flow. Indeed, as observed in the glass tube condenser tested, in sections of the loop where the ratio of inertial and viscous forces (gravity, acceleration, fluid shear, etc.) to surface-tension forces was low, the "slug-flow regime" predominated; that is, the liquid tended, in response to surface-tension forces, to bridge the duct and form a series of liquid slugs. These slugs were then forced into the all-liquid region by a "piston" effect as the vapor bubbles trapped between the slugs condensed to liquid (see fig. 1).

The stability of this slug-flow regime is an important factor in choosing the inside diameter of the condensing duct for a capillary-pumped heat-transfer loop. If a loop must be tested in a 1-g environment, it is desirable to choose a duct diameter small enough so that gravity forces will not cause the condensate to puddle in the bottom on the duct, but will promote the formation of liquid slugs to be transported downstream by the loop pressure drop approximately as shown in figure 1. A loop with its tubing sized in this manner will perform almost as though it were in a zero-gravity environment if the loop tubing is confined to an approximately horizontal plane. Using this criterion, all the tubing used in the test loops for this report had inside diameters of less than 0.2 inch.

Working-Fluid Requirements

The performance of a capillary-pumped heat-transfer loop is also dependent on the characteristics of the working fluid. The fluid should have a high latent heat of vaporization so that large quantities of heat may be transferred with a minimum fluid flow rate. The surface tension of the fluid should be high so that adequate evaporator pressure differences can be obtained without resorting to a wick with excessively small pores. The fluid vapor density should be as high as possible to keep vapor velocities, and thus, vapor pressure drops, to a minimum. A low vapor viscosity will also reduce the vapor pressure drop.

The presence of noncondensable vapors may adversely affect the performance of capillary-pumped loops of the type tested. Such vapors lower the efficiency of the condensing mechanism and, since all vapor bubbles in the loop are trapped or filtered out upstream of the wick, cause blockage of the duct feeding liquid to the wick. However, with proper design of the liquid leg portion, the loops can be made insensitive to small volumes of noncondensables. To avoid the generation of noncondensable vapors, the working fluids should be chemically stable, noncorrosive to the loop structure, and resistant to breakdown by radiation.

APPARATUS AND PROCEDURE

Selection of Working Fluid and Configuration

Water was selected as the working fluid for the experiments because of its good performance and its obvious convenience. However, it was realized that to operate water-filled loops in the temperature range near 500° F (where the performance of water is near its maximum) the loops would have to be designed for high pressure (~681 psia). Because of this pressure requirement, a tubular geometry seemed advantageous. The tubular geometry, in addition to being an efficient pressure container, also seemed to lend itself to incorporation in "shell-and-tube" heat exchangers for cooling fluids, as well as for the contact cooling of solids.

Test Loop 1

Evaporator. - Figure 3 shows the details of evaporator 1. In general, the evaporator consisted of a 1-inch outside-diameter copper tube with 10 internal, longitudinal fins about 5 inches long. One end of the 1-inch outside-diameter tube was reduced to a 3/8-inch outside-diameter tube to serve as the vapor outlet. The opposite end of the 1-inch outside-diameter tube was fitted with a sealed end cap mounting a perforated 3/16-inch outside-diameter coaxial tube at its center. This 3/16-inch tube served as the liquid injector for the evaporator wick.

The wick tube for this evaporator was made from a quartz felt insulation material with a basic fiber diameter of 0.00005 inch (1.3 μ). A rectangular piece of the quartz felt was rolled around the injector tube and sealed at the injector tube ends with wraps of glass fiber cord. Then, the injector and wick assembly was inserted into the copper shell and the end cap nut was installed to seal the shell into a pressure-tight container.

The evaporator was heated electrically with a sheathed heating wire wrapped around the copper shell (fig. 4). The input heat load was conducted to the wick surface by the internal fins of the shell (see fig. 3). The vapor evolved from the hot-wick surface flowed along the channels between the internal fins, and out the evaporator exit tube into the glass condenser tubing. The liquid condensate from the condenser tubing flowed back into the injector tube, radially outward through the wick, and was again vaporized from the hot-wick surface.

Condenser. - The glass condenser tube used with evaporator 1 permitted the study of the condensate flow mode and helped determine the tube size and length for the evaporator 2 condenser. Much of the condenser detail is visible in figure 5. The 95 feet of 0.193-inch inside-diameter glass tubing had six outlet taps to permit the selection of six

different active condenser lengths (17 to 100 ft).

The loop was instrumented with thermocouples to indicate the evaporator inlet liquid temperature, the evaporator outlet vapor temperature, and the evaporator outer surface temperature. The test loop contained two pressure transducers, one to measure the absolute loop pressure and one to measure the pressure differential across the evaporator. The input power to the evaporator heater was measured with a precision wattmeter.

The instrumentation was intended to monitor the loop mechanisms, rather than to study any specific performance detail. The thermocouples were not calibrated, and, in general, interpretation of the data was limited to the definition of operational trends.

Test procedure. - Evaporator 1 loop was operated at constant pressure with a variable condensing vapor length. If the volume of water in the air trap flask (fig. 5) is considered as part of the loop volume, then the volume of the loop was varied, in effect, by allowing liquid water to flow into or out of the air trap flask (i. e., the flask acted as a constant pressure liquid accumulator). As the evaporator power input was increased, liquid flowed out of the loop into the air trap to maintain the loop pressure constant. When the input power was reduced, liquid would return to the loop to again maintain constant pressure. Essentially, the condensing vapor leg was allowed to expand or contract to adjust to an increase or decrease, respectively, in power input.

The evaluation of evaporator 1 loop was conducted at a nominally constant loop pressure of 18.4 pounds per square inch absolute, resulting in the evaporator exit vapor temperature being maintained at 223° F by the mechanism described in the preceding paragraph. At input powers below 283 watts, operation of the accumulator (air-trap flask) pressure control was not feasible. Therefore, loop 1 was not tested at powers less than 283 watts. The maximum evaporator power input was 823 watts. Several attempts to exceed 823 watts, by any significant amount, interrupted the pumping mechanism - probably because the evaporator wick bubble pressure had been exceeded.

Test Loop 2

Evaporator. - Evaporator 2 had the same general geometry as evaporator 1, but in detail was quite different. As shown in figure 6, evaporator 2 was made from 1-inch outside-diameter nickel tubing with an 0.035-inch-thick wall. Into this 1-inch tube was furnace brazed a machined-nickel vapor vent structure (see fig. 7). A transition cone on the liquid inlet end of the evaporator supported a 1/4-inch outside-diameter perforated liquid injection tube located coaxially to the 1-inch nickel container tube. A counterflow configuration was incorporated into the liquid injector tube to permit thorough purging of noncondensable gas. The vapor end of evaporator 2 was closed by an O-ring sealed flange that provided an opening in the assembly for installing the wick structure. As with evap-

orator 1, the wick of evaporator 2 was made of quartz felt, but instead of being formed of a single rolled piece of felt, wick 2 was built up from many disks punched from the quartz felt "bat." A few sample wick disks are shown in figure 7. The head flange (fig. 6) extended into the evaporator to maintain a pressure on the wick disks, and also provided a vapor outlet fitting for the evaporator (see fig. 6).

The heater of evaporator 2 was similar to that of evaporator 1 in that it consisted of 40 turns of sheathed heater wire helically wound on the outer surface of the 1-inch container tube.

Condenser. - The condenser tube for evaporator 2 loop was made of 52 feet of 1/4-inch outside-diameter (0.180-in. i.d.), 0.035-inch-wall, 304 stainless-steel tubing. Figure 8 shows the entire loop mounted on an aluminum frame. The straight runs of condenser tube were 5 feet long with a centerline spacing of 2 inches. Figure 9 shows some of the loop component detail. The entire loop was electrically insulated from the support frame to allow the condenser tube to be resistance heated (by passing electric current through the tubing with a low-voltage transformer) during the purge and fill operation.

Test procedure. - The operation of evaporator 1 loop had emphasized the need to minimize the concentration of noncondensable gas in capillary loops to reduce the tendency of the feed liquid leg to separate from the wick inlet. To accomplish this gas-free fill operation for loop 2, the loop was purged with low-gas-content steam for a period of 2 to 3 hours, and finally filled with a single batch of steam condensate from a glass reboiler. A schematic drawing of the important loop and fill system components is presented in figure 10.

The temperature instrumentation for loop 2 was essentially the same as for loop 1, but no pressure transducers were used in order to avoid the valves and fittings required for pressure instrumentation. As with evaporator 1, the power input to evaporator 2 was recorded from a precision wattmeter.

To avoid any leakage of air into the loop, the loop pressure was always maintained above atmospheric pressure. Thus, the low end of the operating range was characterized by an evaporator power input of 600 watts, a saturation pressure of about 15.6 pounds per square inch absolute, and a saturation temperature of 215° F. To ensure the integrity of the evaporator heater, the input power was limited to a maximum of 1000 watts, which resulted in maximum test range conditions of 58.4 pounds per square inch absolute loop pressure and 291° F loop saturation temperature.

In contrast to the operation of loop 1, loop 2 was operated in the constant volume mode with no variable volume liquid accumulator included in the system. As a result, the pressure and temperature of loop 2 varied with the input power. Of the total loop length of 52 feet, about 5 feet were filled with liquid, leaving a vapor leg length of approximately 47 feet. One characteristic of this constant fluid volume loop was that the vapor length also remained essentially constant over the test range. This would be expected

because only small mass exhanges between the liquid and vapor phase would accommodate large changes in loop operating pressure.

To check the power capacity of loop 2 the evaporator was operated in the power range between 600 and 1000 watts. During a period of about 2 hours, the power input was step-changed between 600 and 1000 watts (15 min segments at each of the two power levels) to test the stability of the loop to sudden load changes.

The sensitivity of the loop to the direction of gravity was checked by operating the loop in three nonhorizontal positions, as documented by figure 11. During these orientation tests, the evaporator input power was 700 watts.

RESULTS AND DISCUSSION

Loop Performance

General performance. - Figure 12 shows a selection of test variables for loop 1 plotted as functions of the evaporator input power E. The dependent variables plotted are the condensing vapor leg length (measured), the static pressure rise across the evaporator ΔP_e (measured), the water flow rate m (computed), and the condenser inlet Reynolds number Re (computed). The water flow rate and the Reynolds number were computed using the expressions

$$m = \frac{E}{h_{fg} + C_p \Delta T_\ell} \tag{1}$$

and

$$Re = \frac{4m}{\pi D_t \mu_v} \tag{2}$$

where

h_{fg} latent heat of vaporization of working fluid, Btu/lb mass

C_p specific heat of subcooled feed liquid, Btu/(lb mass)(^oF)

ΔT_ℓ difference between loop saturation temperature and evaporator inlet liquid temperature, ^oF

D_t inside diameter of condenser tube, ft

μ_v dynamic viscosity of condenser inlet vapor, (lb force)(sec)/ft^2

Since coaxial evaporator 1 was well insulated during operation, the heat loss from the outer evaporator surface was neglected.

The shapes of the curves presented in figure 12 reveal most of the important characteristics of loop 1. The water flow rate m varied almost linearly with input power. This would be expected since, in equation (1), the heat of vaporization h_{fg} was constant over the test range and the variation of the $C_p \Delta T_\ell$ term changed the value of m a maximum of 2 percent.

The Reynolds number curve was linear because of its linear dependence on m. Likewise, the vapor leg length was a linear function of m since the heat rejection (15.2 W/ft tube length), and thus, the condensate formation rate, was almost constant along the entire vapor leg. (The constant pressure operation of the loop also tended to maintain a constant tube temperature for the vapor leg, regardless of its length.) The approximately parabolic shape of the ΔP_e curve indicates that the condenser tube flow regime was turbulent, a conclusion supported by the fact that, at the datum point of maximum m, the condenser inlet Reynolds number was 6550. It is significant to note that the process of distributing 824 watts of thermal power into a vapor leg 55 feet long and 0.193 inch in diameter required a pumping pressure head of only 1.17 pounds per square inch differential. The power density through the outer evaporator surface had a maximum value of 51.4 watts per square inch (25 300 Btu/(hr)(ft^2)), while the power density through the condenser tube inner wall was constant at about 2.09 watts per square inch (1027 Btu/(hr)(ft^2)).

The general performance of test loop 2 was somewhat better than that of loop 1. Evaporator 2 could absorb 1 kilowatt of power at an outer surface density of about 60 watts per square inch and provide sufficient fluid pumping power to distribute this heat load through a 52-foot closed loop of 0.180-inch inside-diameter tubing. Because test loop 2 contained no pressure instrumentation the pressure differential across evaporator 2 is not known.

Evaporator boiling surface performance. - If T_s is the average temperature of the evaporator heat input surface and T_o is the evaporator outlet saturation temperature, the curves in figure 13 relate the thermal power density through the input surface to the temperature difference $T_s - T_o = \Delta T_e$. This temperature drop ΔT_e is a penalty the system designer must "pay" when using the loops for the transfer of heat. In other words, heat is put into the loop through a surface at temperature T_s and rejected from the loop through a surface at a temperature approximately equal to the temperature T_o of the condensing vapor. Obviously, to minimize the surface area required for heat rejection from the loop, the temperature drop ΔT_e must be minimized. Of course, ΔT_e does not include the temperature drop from the bulk condensing vapor to the heat sink because this latter temperature drop is a complex function of the heat sink design and environment.

Figure 13 shows plots of ΔT_e for both test evaporators. Evaporator 2 was tested

with two different wick packings, one with 107 quartz disks and one with 134 disks. The performance of evaporator 2 with the 107 disk wick was the best of this test series with an almost constant value of 1.67 watts per square inch per ^{o}F of ΔT_e. However, the performance of evaporator 2 with the 134 disk wick was inferior (greater ΔT_e for a given power density) to that of the other evaporator configurations. The cause of this wide variation in performance of evaporator 2 is not known. However, it is possible that the variation was the result of a partial blockage of the evaporator vapor vent ducts by fragments of wicking torn off during the wick installation. Such blockage could cause patches of the wick boiling surface to dry out, thus increasing the average ΔT_e required for operation at a given power level. The hysteresis characteristic of the 134 disk curve in figure 13 could have been caused by the gradual clearing of the wick fragments by the vapor flowing from the evaporator. This clearing action is supported by the fact that wick fibers were commonly observed deposited outside the evaporator in fittings and valves in the condensing portion of the loop (following a period of loop operation).

In general, it may be said that the particular form of quartz felt used for wicking, although it exhibited excellent wicking performance, had poor resistance to erosion by the working fluid. Also, the hand-packing technique for installing the wick resulted in poor repeatability of wick characteristics.

Power transient tests. - Loop 2 showed no sign of instability in responding to the power input steps from 600 to 1000 watts (one step, both increasing and decreasing). The time constant (the time for 63 percent of the total change) of the loop temperature response was about 2 minutes. Thus, a wide and sudden variation in input power seems to present no fundamental problem that might lead to a cessation of fluid pumping in a capillary-pumped heat-transfer loop of the type tested.

Gravity sensitivity tests. - Since a capillary-pumped heat-transfer loop is passive in the sense of requiring only waste heat to cross its boundaries, the most important performance criterion to be observed external to the loop by a systems engineer is whether or not the loop is operating with a normal temperature distribution around the flow duct. During the orientation testing of loop 2, its performance was monitored by comparing the temperature values during horizontal operation with those recorded for other loop attitudes. After testing loop 2 in the positions shown in figure 11, it was concluded that the ΔT_e of the evaporator boiling surface was essentially invariant with an orientation change. This meant that the evaporator liquid-feed and boiling mechanisms of this loop were controlled by capillarity, even in the 1-g environment.

The fact that the loop operated well on end (fig. 11(c)) indicates that some effective method of condensate transport prevented the liquid from accumulating in the lower bends of the vertically positioned loop. It is interesting to note that during this run (fig. 11(c)) the condensed water temperature was 220^{o} F, resulting in a surface tension σ of about 0.004 pound per foot. Thus, the capillary head in the 0.180-inch inside-diameter con-

denser tube (assuming zero contact angle) was $4\sigma v_f/D_t = 0.21$ inch, where v_f is the specific volume of 220° F liquid water. The vertical rise in the loop positioned as shown in figure 11(c) was about 62 inches. Therefore, whatever the actual mode of condensate transport in the condenser, the liquid was moved a vertical height of almost 300 times the capillary head of the liquid in the tube.

It is proposed, but not proven, that the condensate transport mechanism during the vertical operation of loop 2 was a combination of (1) a wall film of liquid driven along by fluid shear coupling to a central vapor core, and (2) the condensate slug flow mechanism introduced in the section PRINCIPLE OF OPERATION. Transport mode (1) would predominate near the condenser inlet where the vapor velocity is high and the condensate inventory low. Mode (2) should predominate near the condensing vapor-liquid interface where the vapor velocities are low and the liquid inventory is large. Whatever the true mechanism of condensate transport, capillary-pumped evaporators of the type investigated can probably be "checked-out" in 1g to determine their general zero-gravity performance characteristics.

Problems with noncondensable gas. - Any noncondensable gas in the evaporator 2 loop was very detrimental because the loop was operated at constant volume, as was explained in the section APPARATUS AND PROCEDURE. In such a constant volume loop, even a small gas bubble can expand into a large void if the loop saturation pressure is permitted to drop to a very low value. These large voids can block the flow of liquid through a smooth-wall liquid subcool tube by the mechanism illustrated in figure 14. If such blockage occurs, the loop stops operating. It is possible that a secondary wick layer of sufficient length attached to the inner wall of the liquid leg tube would permit adequate bypass of liquid around the gas bubbles. However, the effectiveness of this modification was not evaluated in the tests reported here.

The first problems associated with noncondensable gas in the loops were encountered during the working-fluid fill operations. The water fill system used for coaxial evaporator loop 2 (i.e., distilling fluid condensate into the loop) seemed to solve the fill operation gas problem. However, elimination of the latter problem was followed by the discovery that internal loop corrosion was generating gas in the working fluid.

After evaporator 2 had been packed with the 134 disk wick and put into operation, it was noted that a gas was collecting in the gas trap (see fig. 9) at a steady rate of about 3 standard cubic centimeters per day. A mass spectrometer analysis of the gas identified it as almost pure hydrogen. When the loop was shut down after the run, the evaporator wick was checked for iron, with positive results. Also, a red-brown residue was observed coating the inner surface of the glass portion of the gas trap. These facts led to the conclusion that the hot stream or liquid water in the loop was slowly reacting with iron-bearing alloys to form iron oxide and free hydrogen gas. Thus, it must be empha-

sized that the materials and working fluids selected for capillary-pumped heat-transfer loops must be completely compatible.

SUMMARY OF RESULTS

The more significant results of an experimental feasibility study of water-filled capillary-pumped heat-transfer loops are summarized as follows:

1. Test evaporator 2 could absorb 1 kilowatt of power at an outer surface density of about 60 watts per square inch and provide sufficient fluid pumping power to distribute this heat load through a 52-foot closed loop of 0.180-inch inside-diameter tubing.

2. The best evaporator boiling surface performance was obtained with evaporator 2 which would absorb about 1.67 watts per square inch per ^{o}F temperature difference between the outer evaporator surface and the evaporator outlet saturated vapor.

3. Since test loop 2 could operate standing on end, some effective condensate transport mechanism prevented liquid from accumulating in the lower bends of the loop. No provision was made to observe the details of condensate transport in the metal condenser tube, but the transport mechanism was probably a combination of wall film flow and, in the low velocity portions of the condenser, slug flow. The capillary head of the condenser tube was about 0.21 inch, while the vertical rise in the loop was about 62 inches, or almost 300 times the capillary head.

4. Capillary-pumped loops of the type tested are sensitive to noncondensable gas in the working fluid. Gas bubbles can block the flow of liquid to the evaporator wick inlet and stop the loop pumping action. Thus, noncondensable gases must be eliminated from the working fluid and the loop structural materials during the loop filling operation, and the loop materials must be completely compatible to avoid the chemical generation of gases during loop operation.

CONCLUSIONS

General consideration of the results of this test program lead to the following conclusions:

1. Useful capillary-pumped heat-transfer loops of the type reported herein are feasible. Moreover, if the loop condenser duct diameter is not too large, the loops operate well in a 1-g environment in almost any position.

2. In a 1-g environment, slugs of liquid can be raised many capillary heads in an inclined or vertical tube, provided only that the capillary head (in the tube) exceeds the

tube diameter. During the testing vertical lifts of about 300 capillary heads were demonstrated.

Lewis Research Center,
National Aeronautics and Space Administration,
Cleveland, Ohio, August 3, 1966,
123-34-02-01-22.

REFERENCES

1. English, R. E.; and Guentert, D. C.: Segmenting of Radiators for Meteoroid Protection. ARS J., vol. 31, no. 8, Aug. 1961, pp. 1162-1164.
2. Gaugler, R. S.: Capillary Heat Transfer Device for Refrigerating Apparatus. United States Patent No. 2,448,261, Aug. 31, 1948.
3. Grover, G. M.; Cotter, T. P.; and Erickson, G. F.: Structures of Very High Thermal Conductance. J. Appl. Phys., vol. 35, no. 6, June 1964, pp. 1990-1991.
4. Cotter, T. P.: Theory of Heat Pipes. Rept. No. LA-3246-MS, Los Alamos Scientific Lab., Mar. 26, 1965.
5. McGinness, H. D.: Capillary Pumping for Closed-Cycle Gas Systems. Research Summary No. 36-10, vol. 1, Jet Propulsion Laboratory, California Inst. Tech., Sept. 1, 1961, pp. 9-13.
6. Laub, J. H.; and McGinness, H. D.: Recirculation of a Two-Phase Fluid by Thermal and Capillary Pumping. Tech. Rep. No. 32-196, Jet Propulsion Laboratory, California Inst. Tech., Dec. 8, 1961.

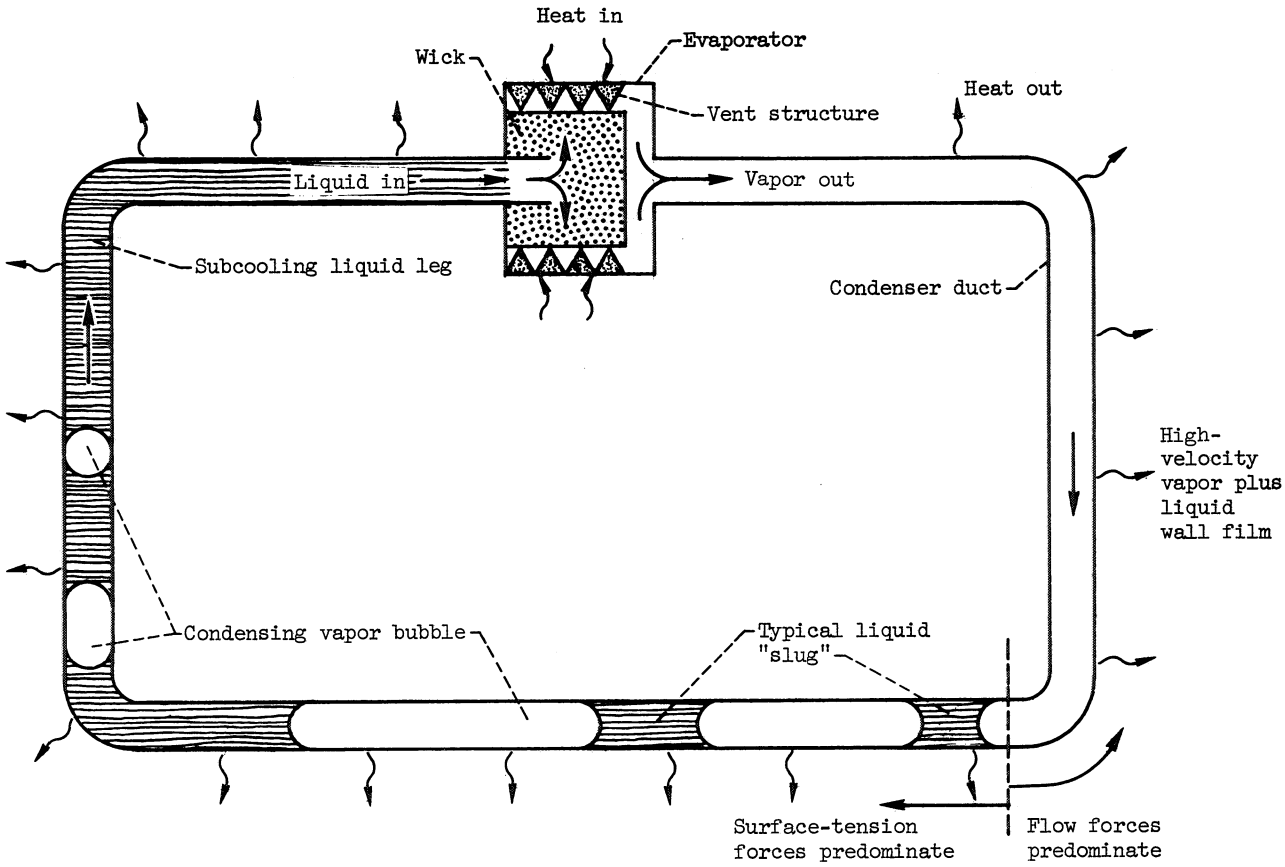

Figure 1. - Capillary-pumped heat-transfer loop showing modes of condensate transport.

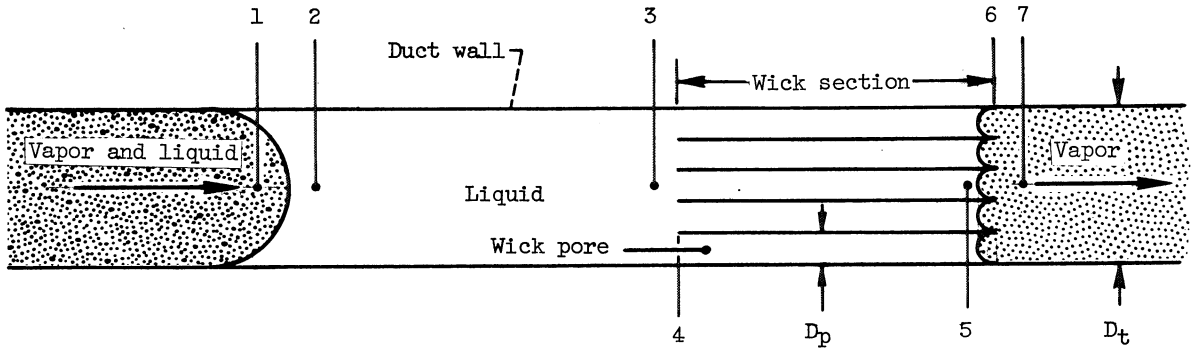

(a) Schematic model of capillary-pumped evaporator.

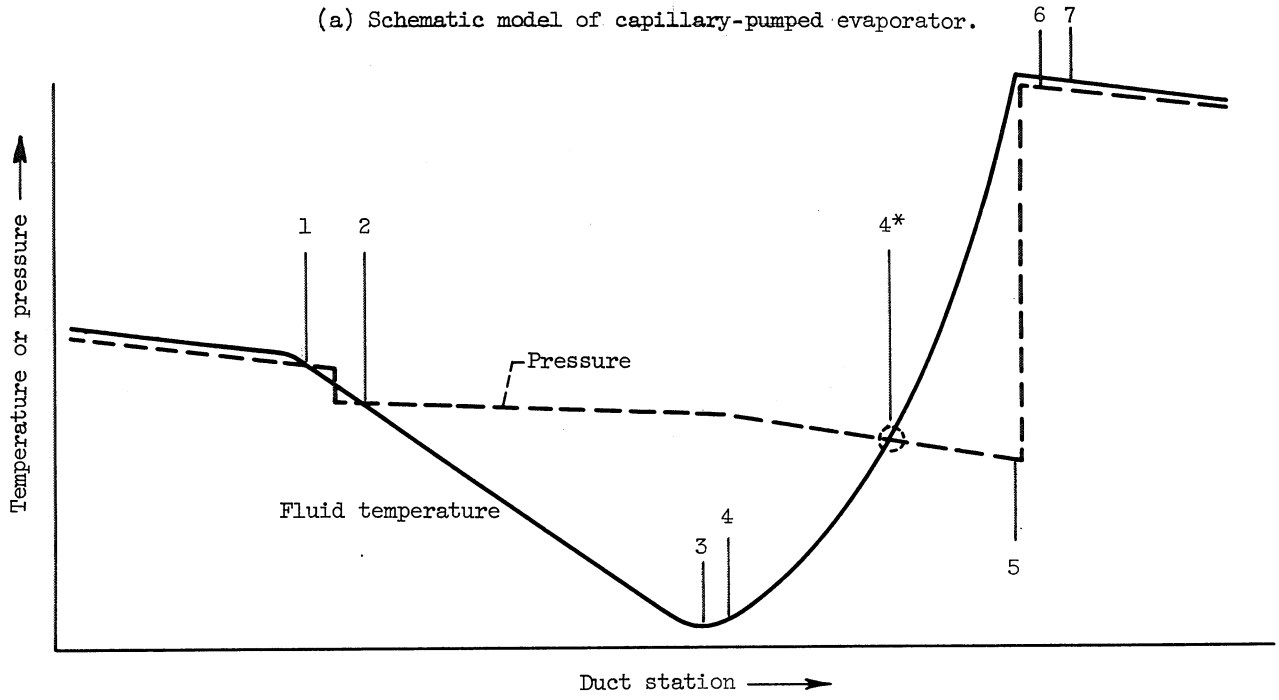

(b) Pressure and temperature profiles.

Figure 2. - Schematic model and pressure-temperature profiles of idealized capillary-pumped evaporator in zero-gravity field.

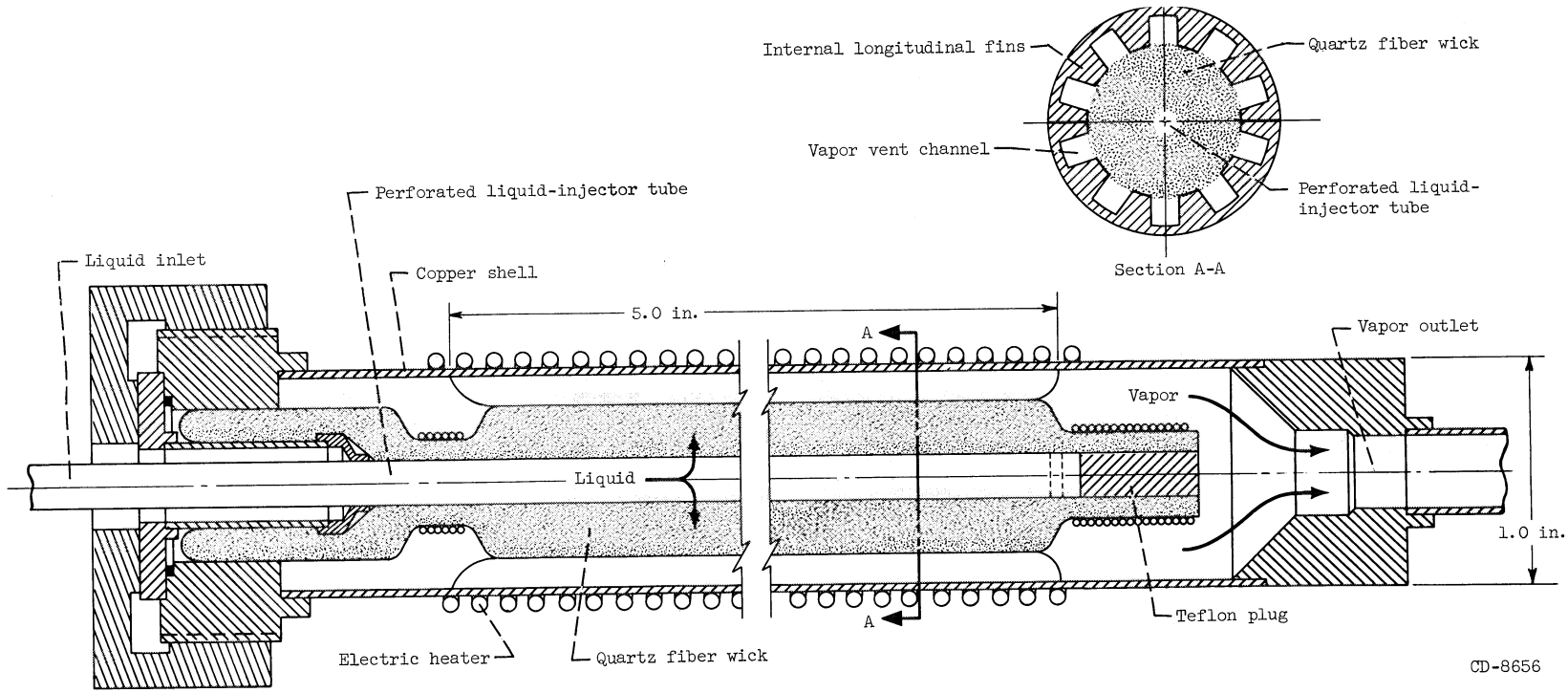

Figure 3. - Design of evaporator 1.

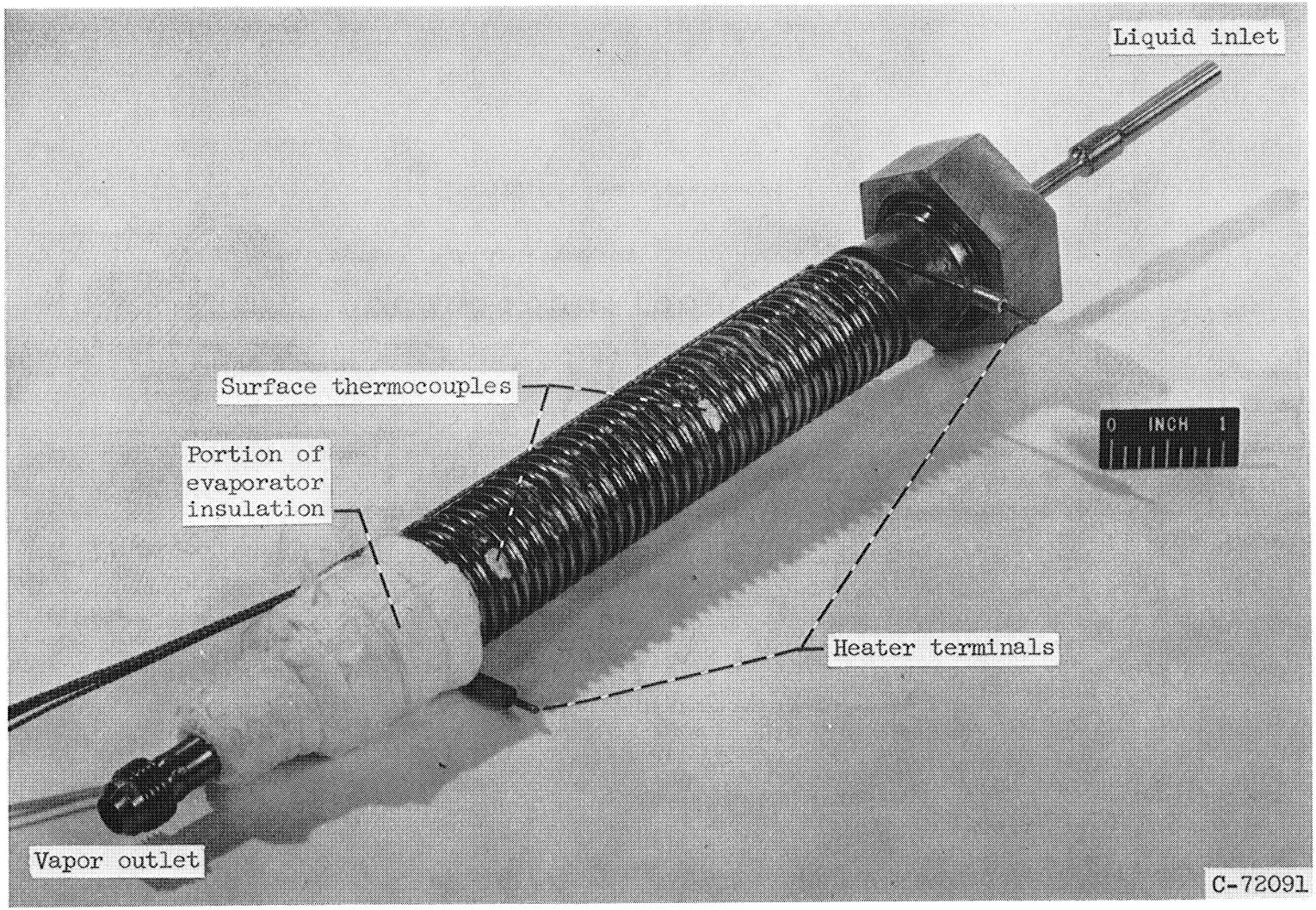

Figure 4. - Evaporator 1 showing electric heater soldered to surface of internally finned copper tube.

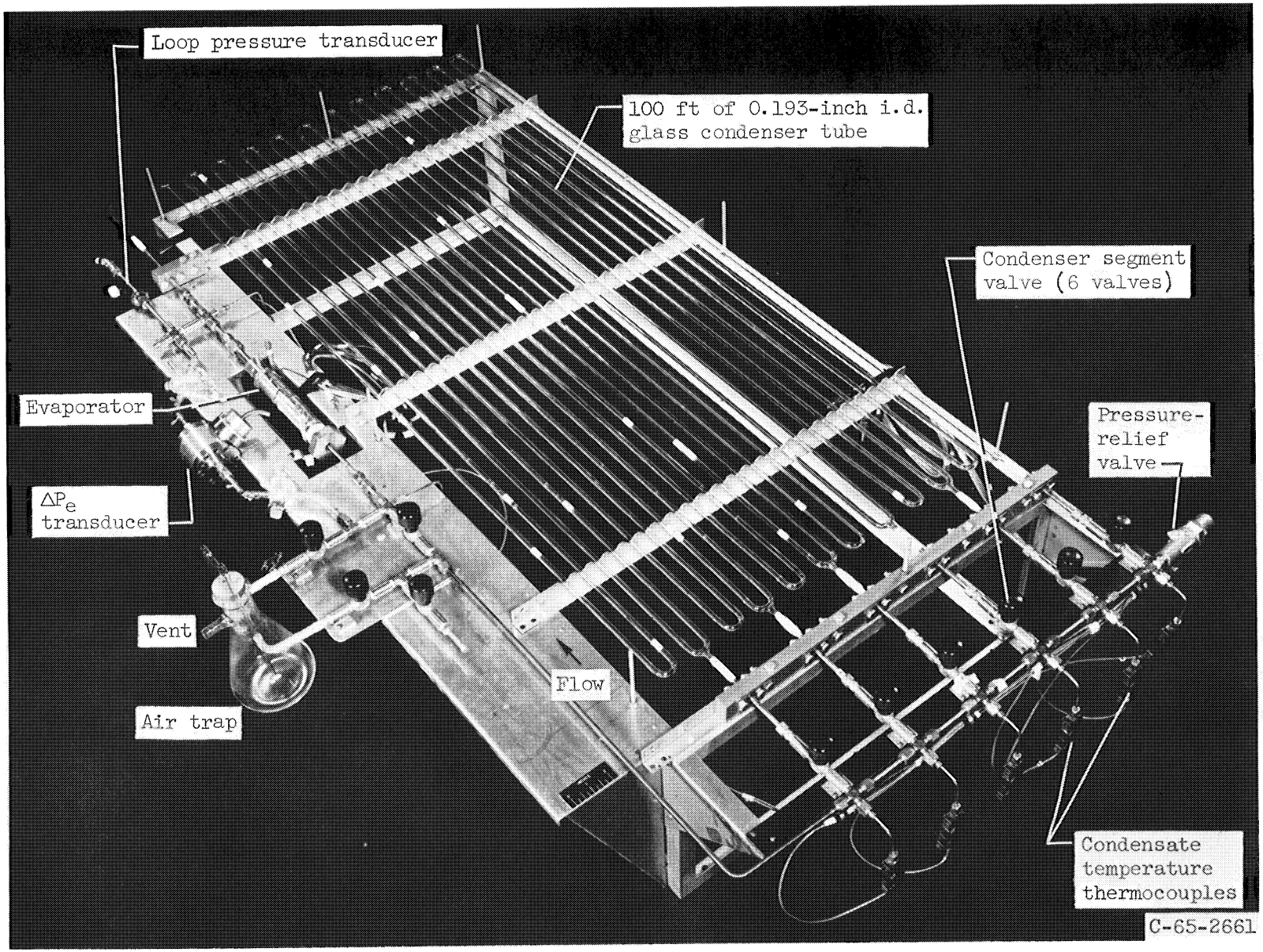

Figure 5. - General layout of test loop 1.

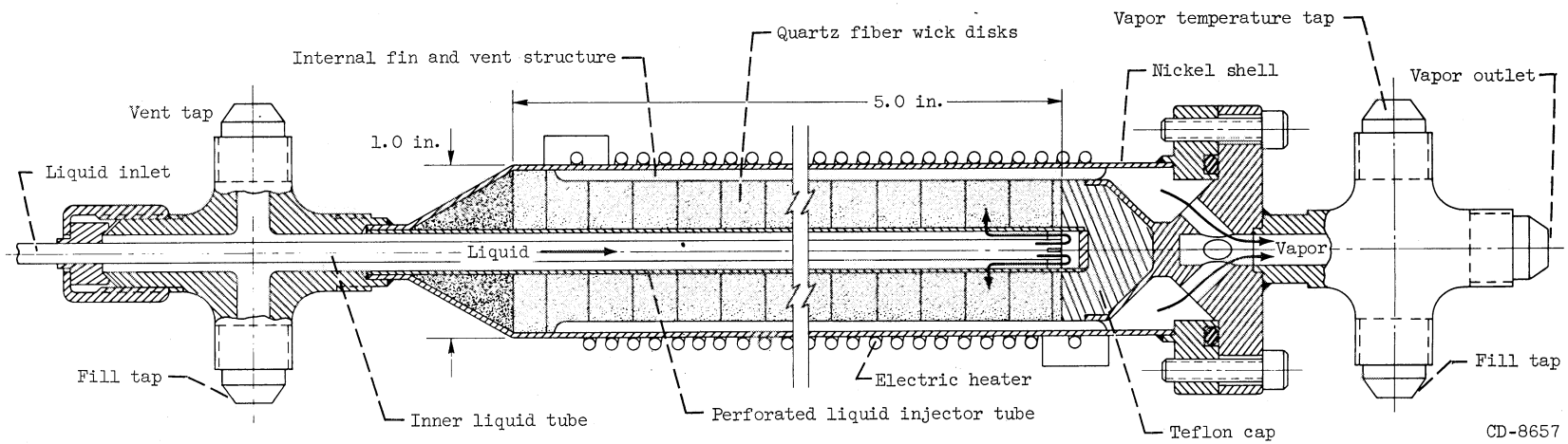

Figure 6. - Design of evaporator 2.

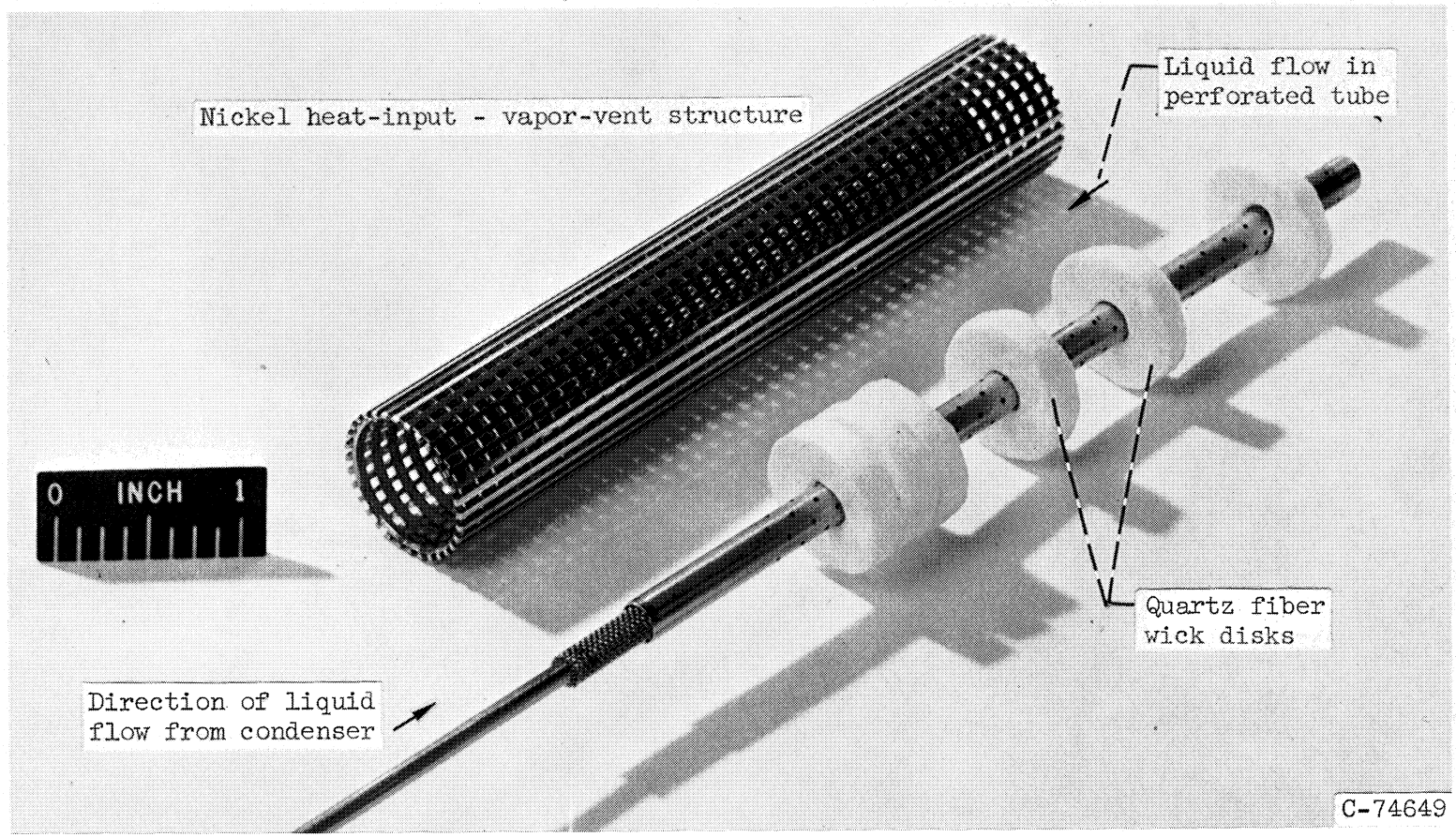

Figure 7. - Detail of heat-input - vapor-vent structure and liquid injector for evaporator 2.

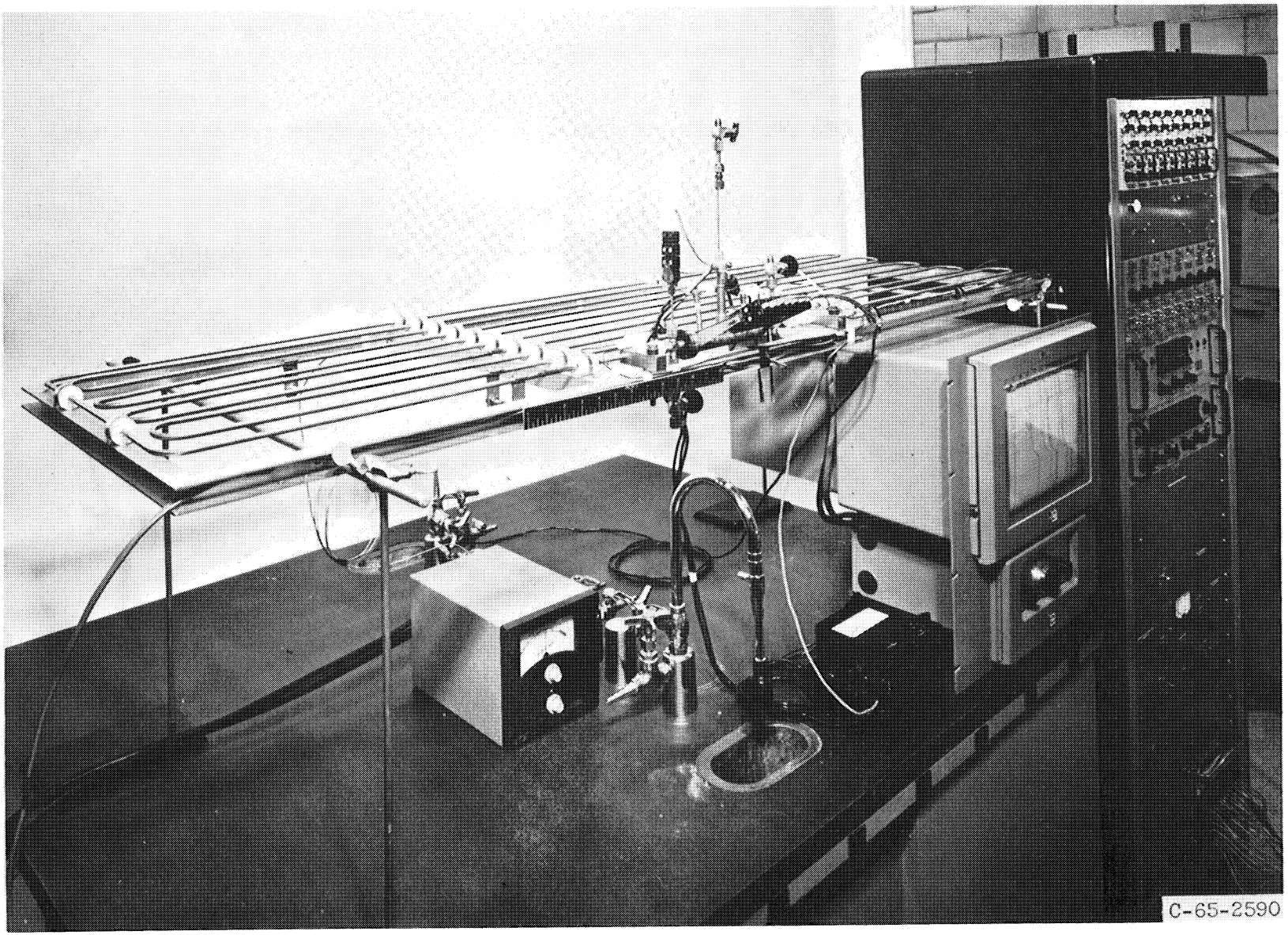

Figure 8. - Test loop 2 operating in a horizontal position with free convection cooling.

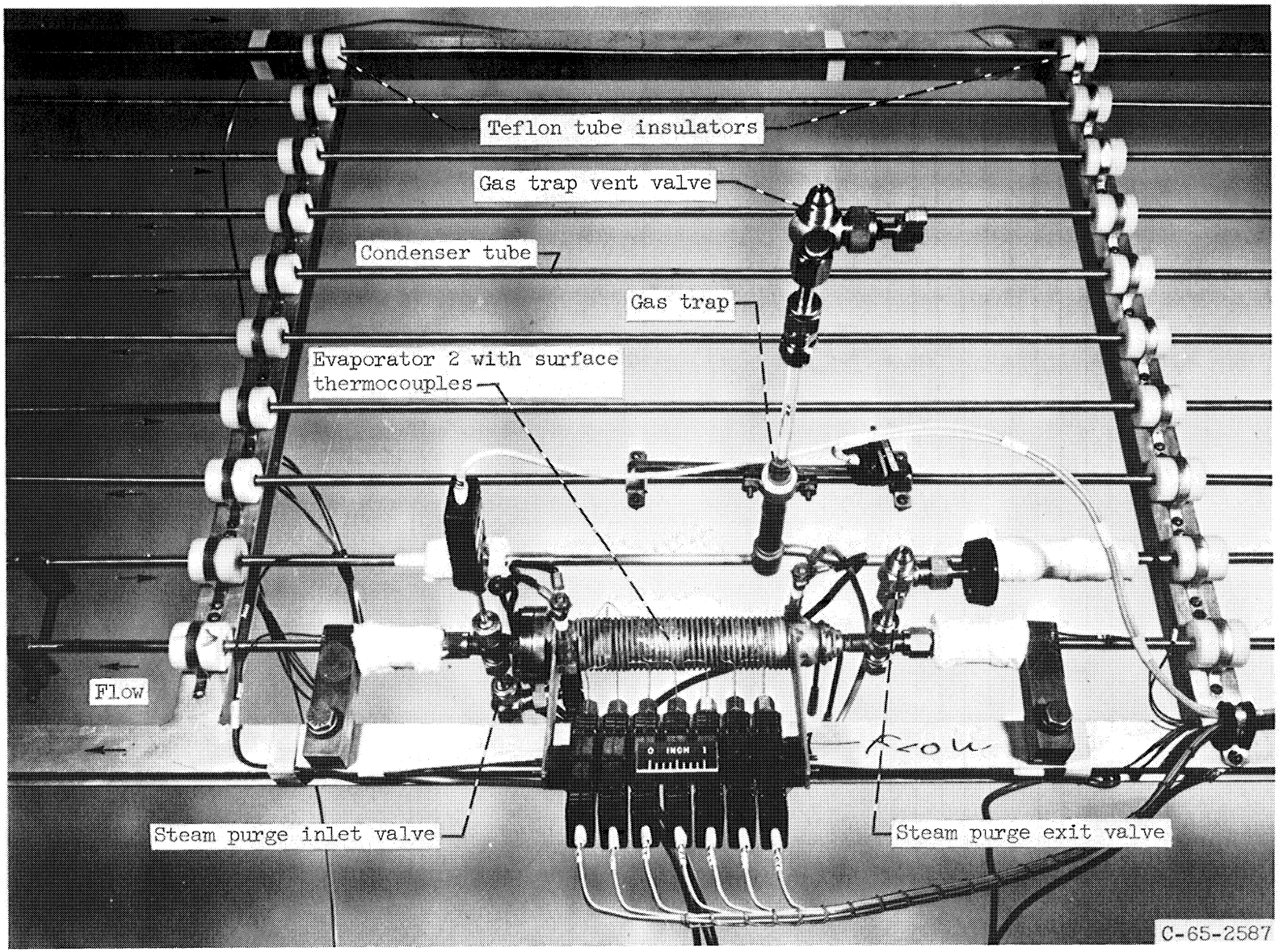

Figure 9. - Detail of test loop 2.

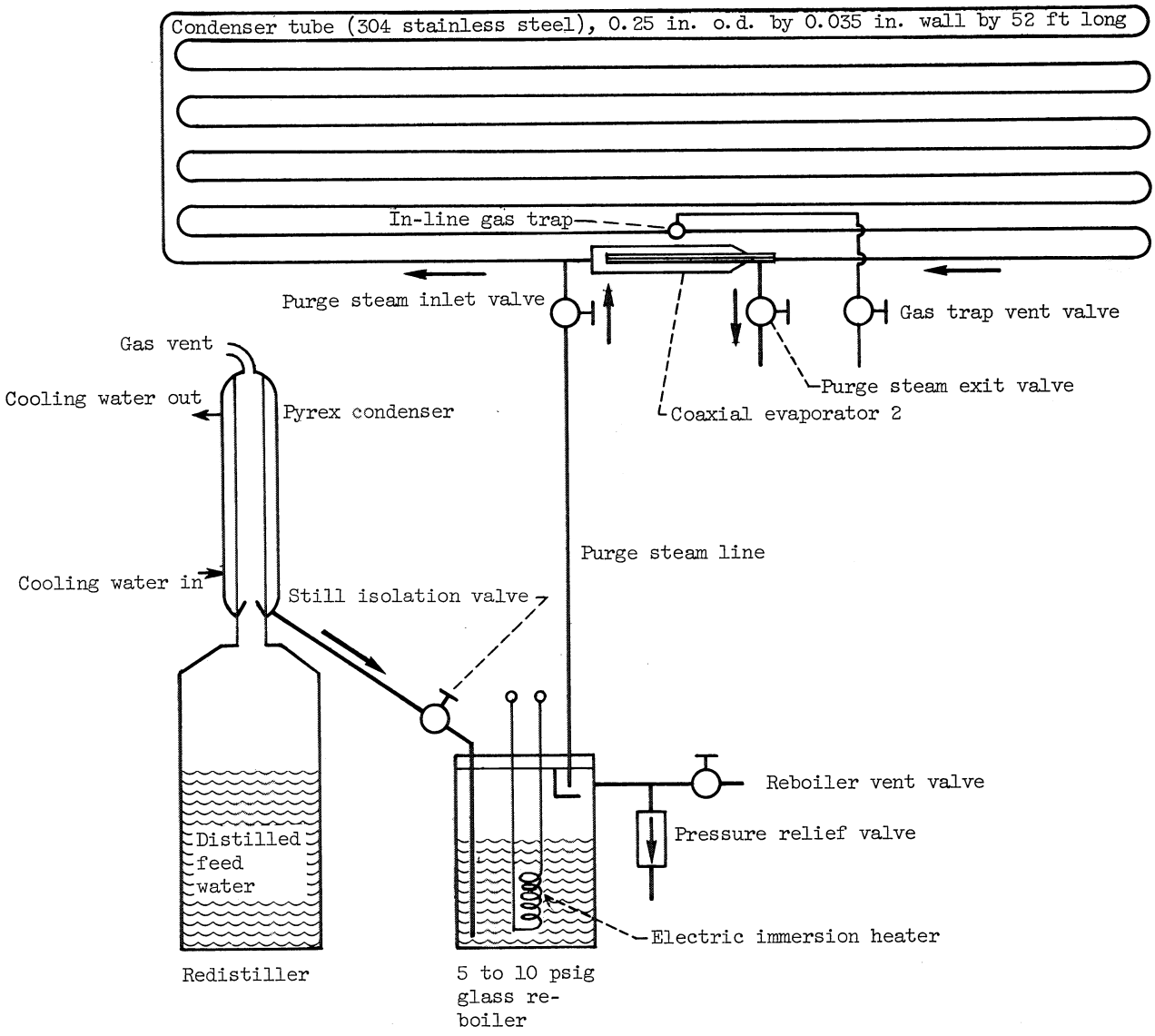

Figure 10. - Schematic drawing of water purge and fill system for test loop 2.

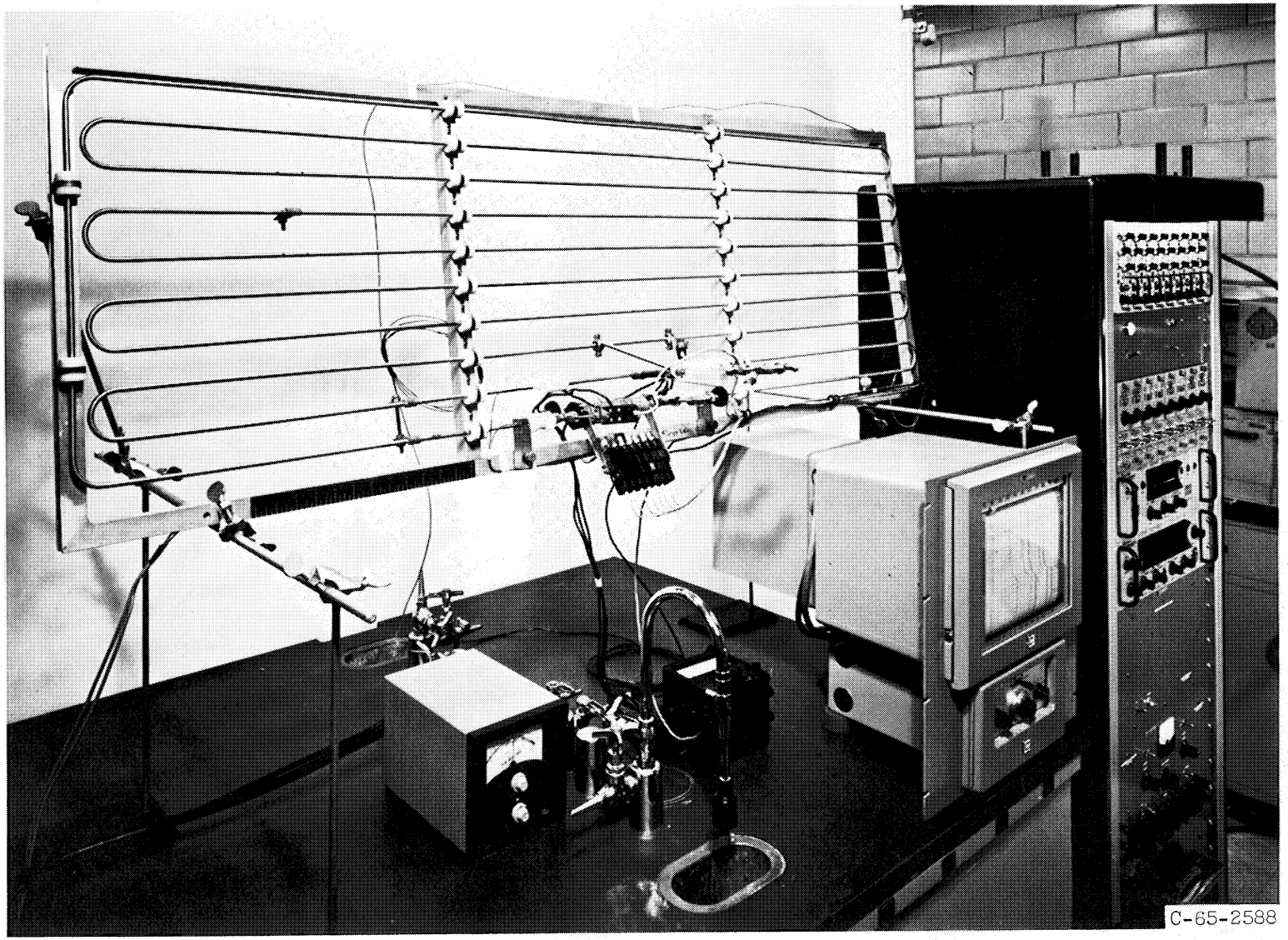

(a) Operating at 700 watts on edge with evaporator at bottom. Gravity aids condensate return to evaporator.

Figure 11. - Test loop 2.

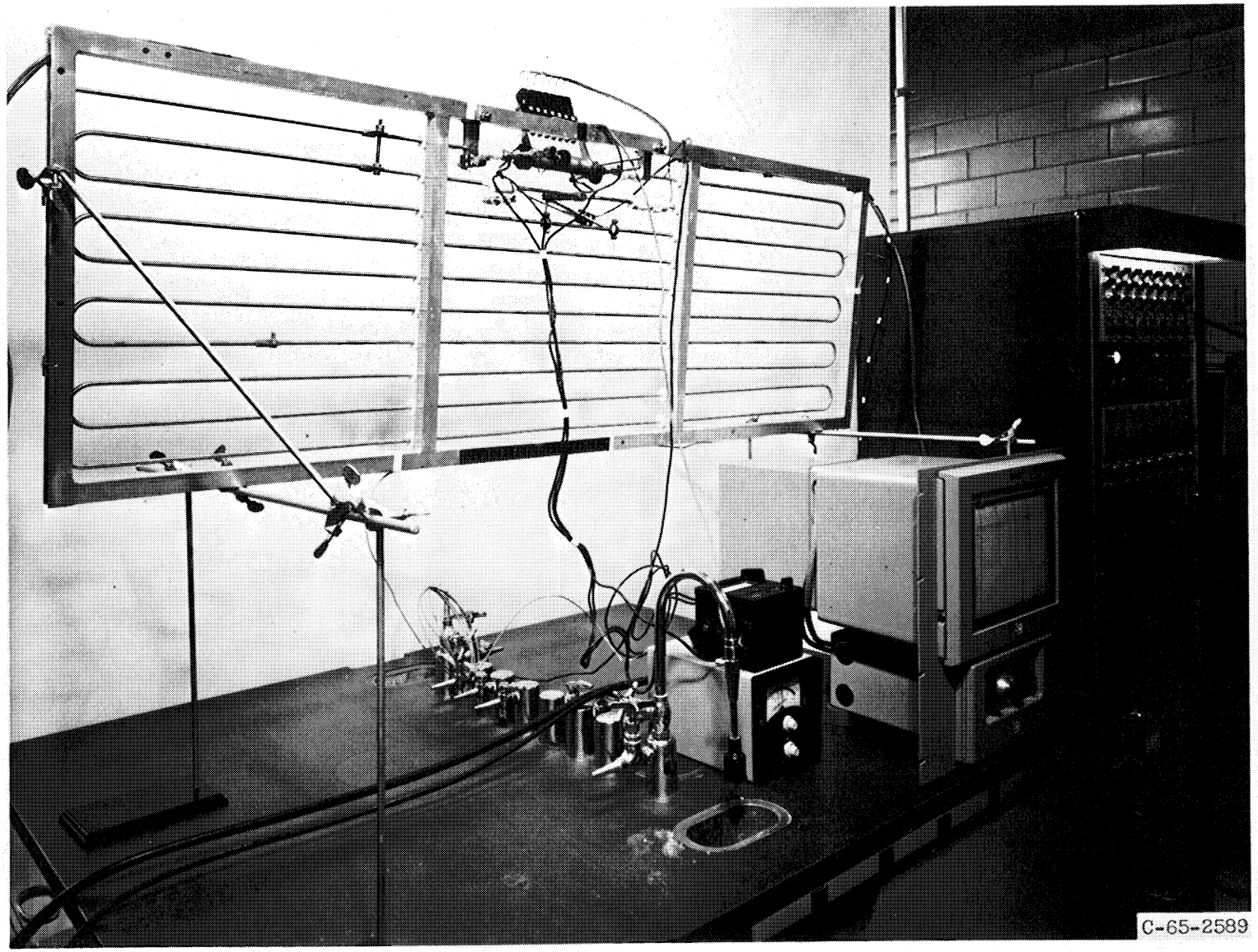

(b) Operating at 700 watts on edge with evaporator at top. Gravity opposes condensate return to evaporator.

Figure 11. - Continued. Test loop 2.

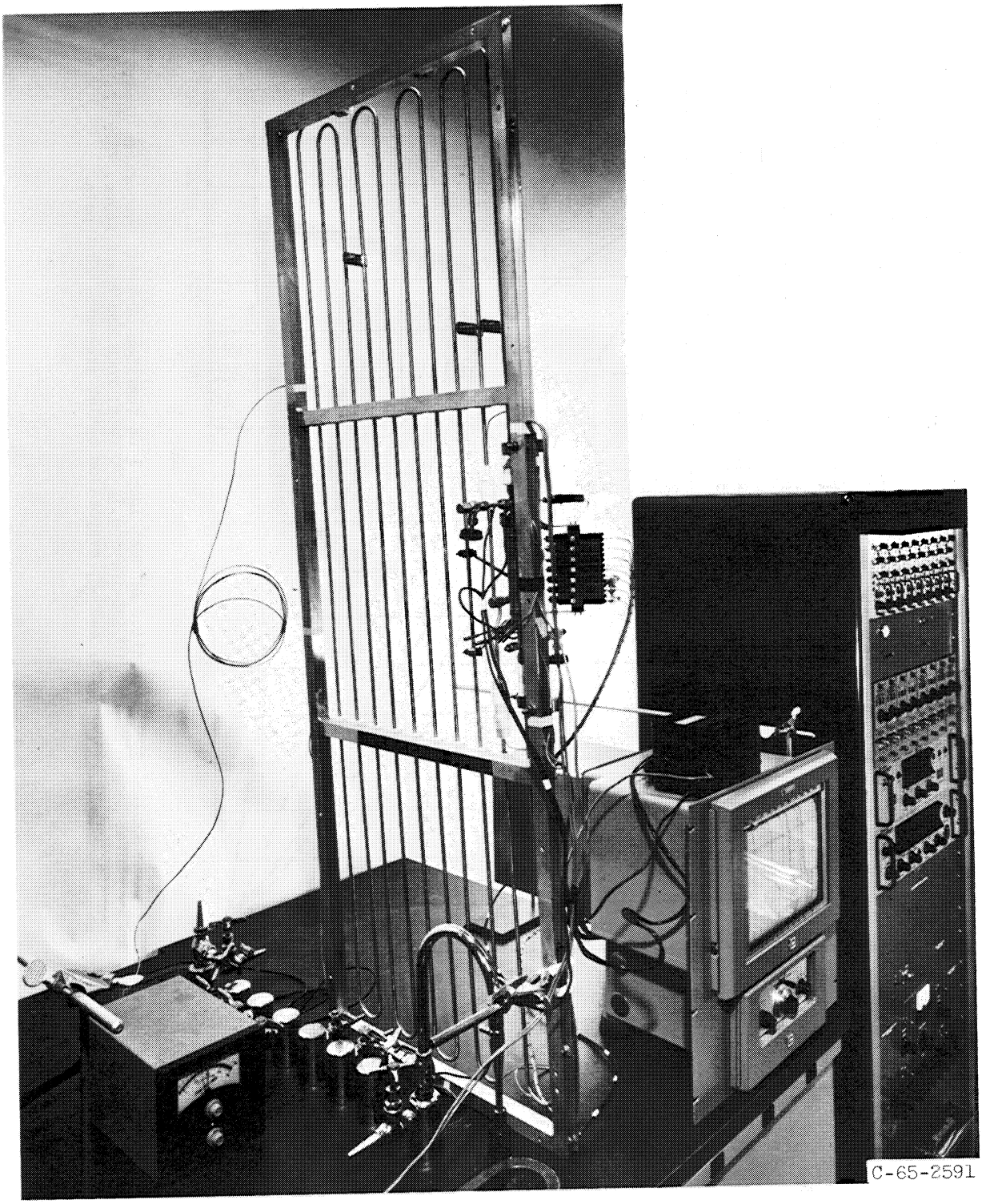

(c) Operating at 700 watts on end with gravity aiding and opposing condensate flow in alternate tubes.

Figure 11. - Concluded. Test loop 2.

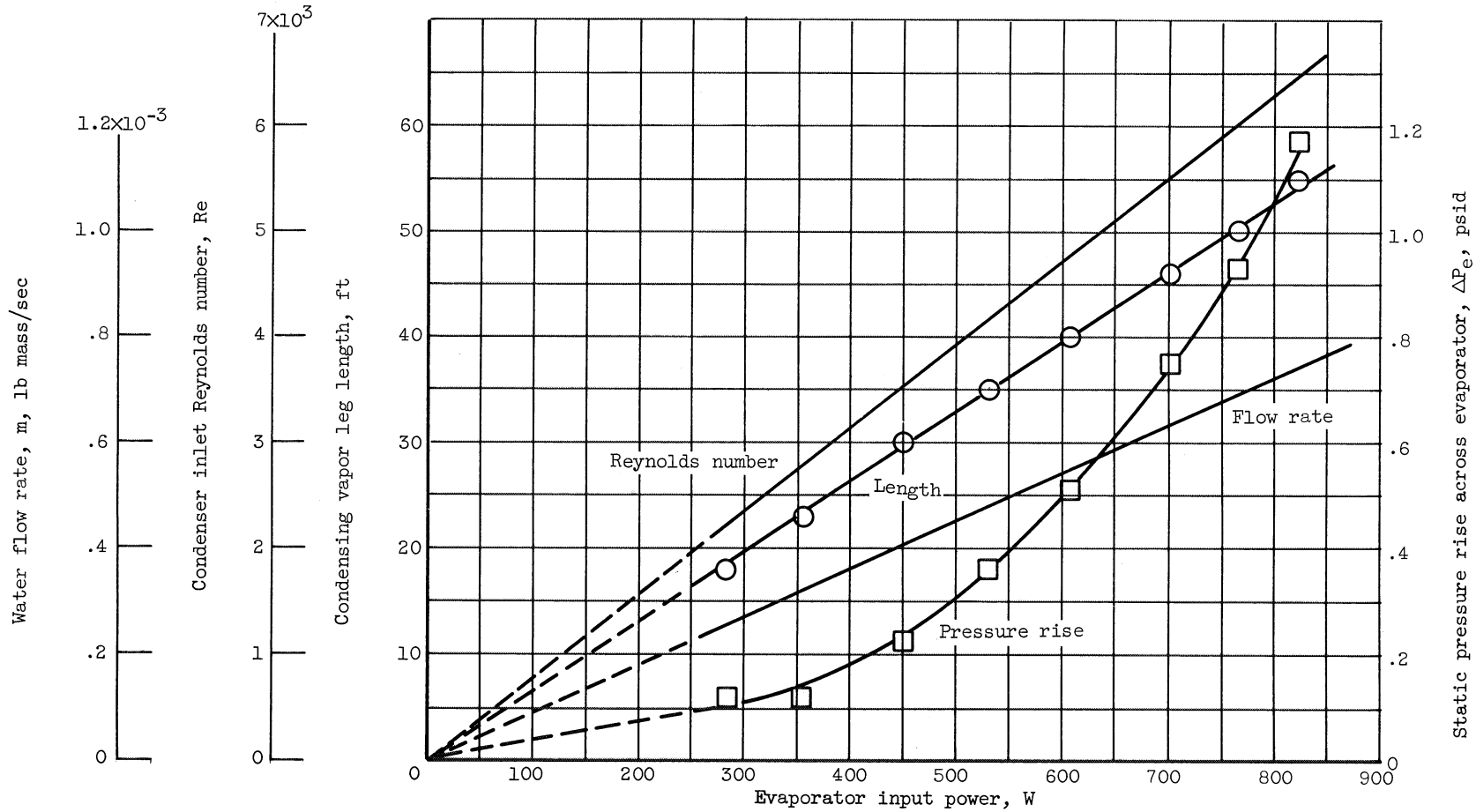

Figure 12. - Typical characteristics of test loop 1 as function of total evaporator input power. Total length of loop (0.193-in. i.d.), 70 feet; room air temperature, 78.8° F; evaporator outlet temperature, 223° F; evaporator outlet pressure, 18.4 psia.

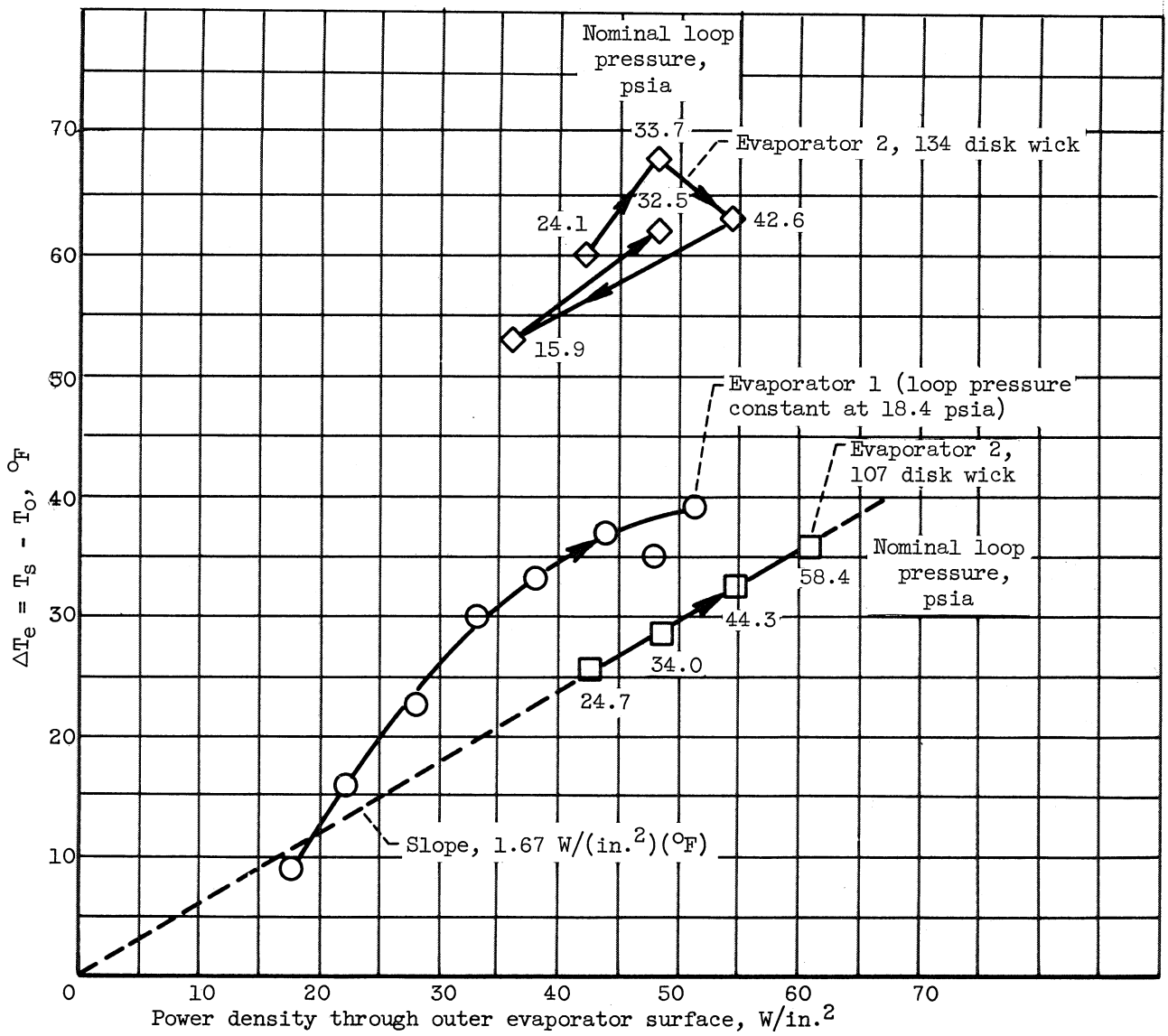

Figure 13. - Temperature difference between outer evaporator surface and evaporator outlet saturated vapor for evaporators 1 and 2 as function of input power density (Arrows on curves denote test sequence.)

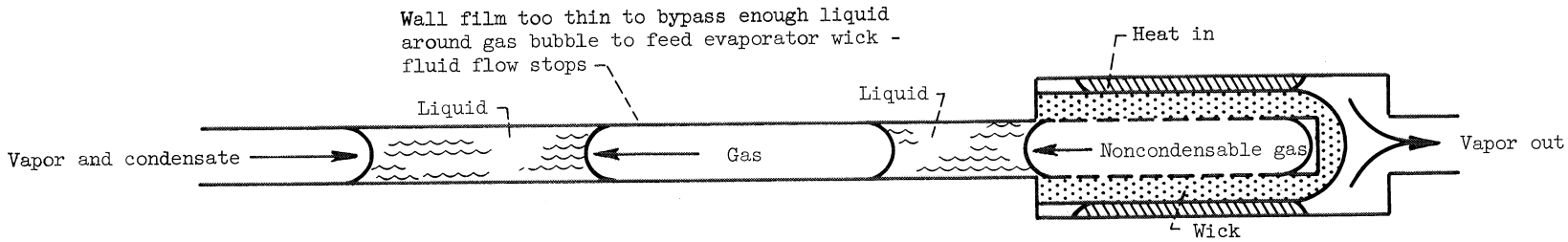

Figure 14. - Capillary-pump failure mechanism caused by excess noncondensable gas in loop.